Cellular/Molecular

Regulation of NLGN3 and the Synaptic Rho-GEF Signaling Pathway by CDK5

Jaehoon Jeong, Wenyan Han, Eunhye Hong, Saurabh Pandey, Yan Li, Wei Lu, and Katherine W. Roche
National Institute of Neurological Disorders and Stroke, National Institutes of Health, Bethesda, Maryland 20892

Neuroligins (NLGNs) are postsynaptic cell adhesion molecules that are involved in synapse assembly and function. The NLGN gene family consists of 5 genes (*NLGN1-3*, *4X*, and *4Y*). NLGN3 forms heterodimers with other NLGNs and is expressed at both excitatory and inhibitory synapses, although the distinct role at different synapses is not fully understood. Cyclin-dependent kinase 5 (Cdk5) is a proline-directed serine/threonine kinase that targets various neuronal substrates to impact neuronal migration, neurite outgrowth, synaptic transmission, and plasticity. Both NLGNs and their presynaptic binding partners neurexins are highly associated with neurodevelopmental disorders. The NLGN3 gene is on the X chromosome and variants in NLGN3 have been linked to the pathophysiology in neurodevelopmental disorders. To better understand the endogenous modulation of NLGN3, we generated an HA-tagged knock-in mouse. We found that Cdk5 associates with NLGN3 *in vivo* and phosphorylates NLGN3 on serine 725 (S725) in the knock-in mouse of either sex. The phosphorylation affects the NLGN3 association with Kalirin-7, a postsynaptic guanine nucleotide exchange factors for Rho GTPase family proteins. We further observed that the phosphorylation modulates NLGN3 surface expression and NLGN3-mediated synaptic currents in cultured rat neurons. Thus, we characterized NLGN3 as a novel Cdk5 substrate and revealed the functional consequences of NLGN3 S725 phosphorylation in neurons. Our study provides a novel molecular mechanism underlying Cdk5-mediated regulation of postsynaptic cell adhesion molecules.

Key words: Cdk5; Kalirin-7; NLGN3; phosphorylation

Significance Statement

NLGN3 is involved in synapse assembly and function at both excitatory and inhibitory synapses and has been associated with the pathophysiology of neurodevelopmental disorders. Cdk5 has brain-specific activity and is involved in neuronal transmission, synapse function, and plasticity. Here, we characterize NLGN3 as a Cdk5 substrate for the first time and show that Cdk5-mediated phosphorylation regulates NLGN3 function. We demonstrate that NLGN3 S725 is a Cdk5 phosphorylation site, and reveal that the site is important for NLGN3 association with Kalirin-7, NLGN3 surface expression, and NLGN3-mediated synaptic transmission.

Introduction

Regulation of cell adhesion molecules is critical for synapse assembly as well as synaptic function. Neuroligins (NLGNs) are Type I membrane proteins on the postsynaptic membrane that mediate synapse formation and maintenance (Varoqueaux et al., 2006). Postsynaptic NLGNs form transsynaptic interactions with neurexins (NRXNs), presynaptic cell adhesion molecules, to form asymmetric synapses (Ichtchenko et al., 1995; Nguyen and Sudhof, 1997; Song et al., 1999; Scheiffele et al., 2000). The NLGN and NRXN transsynaptic interaction triggers recruitment and stabilization of scaffolding proteins, channels, and receptors, for presynaptic and postsynaptic maturation (Scheiffele et al., 2000; Sara et al., 2005; Giannone et al., 2013). NRXNs interact with CASK, and CASK scaffolds presynaptic proteins, such as SynCAM, N-type calcium channels, Mint1, and Veli proteins, which regulate presynaptic release machinery (Biederer et al., 2002; Dean et al., 2003; Spafford and Zamponi, 2003). NLGNs interact with postsynaptic scaffolding proteins, such as PSD-95, which are important for clustering and stabilizing various neurotransmitter receptors, ion channels, cell adhesion molecules, and intracellular signaling proteins in the postsynaptic density (PSD) (Budreck et al., 2013; Giannone et al., 2013; Bemben et al., 2015a; Won et al., 2016; Haas et al., 2018; Jeong et al., 2019). In addition,

Received Dec. 19, 2022; revised Aug. 16, 2023; accepted Aug. 18, 2023.

Author contributions: J.J., W.H., Y.L., W.L., and K.W.R. designed research; J.J., W.H., E.H., S.P., and Y.L. performed research; J.J., W.H., and W.L. contributed unpublished reagents/analytic tools; J.J., W.H., E.H., Y.L., and K.W.R. analyzed data; J.J., Y.L., and K.W.R. wrote the first draft of the paper; J.J. and K.W.R. edited the paper; J.J. and K.W.R. wrote the paper.

This work was supported by the National Institute of Neurological Disorders and Stroke Intramural Research Program.

J. Jeong's present address: Amyloid Solution Inc., Seongnam, 13486, Republic of Korea.

The authors declare no competing financial interests.

Correspondence should be addressed to Katherine W. Roche at rochek@ninds.nih.gov or Jaehoon Jeong at jhjeong@amyloidsolution.com.

https://doi.org/10.1523/JNEUROSCI.2309-22.2023

Copyright © 2023 the authors

NLGNs also bind to gephyrin and other proteins that act at inhibitory synapses (Varoqueaux et al., 2004; Giannone et al., 2013).

The NLGN gene family consists of five isoforms (*NLGN1*, *2*, *3*, *4X*, and *4Y*) and each NLGN isoform displays different subcellular localization and functional effects (Bemben et al., 2015a). All NLGN isoforms show high similarity in amino acid sequence, but each is also precisely regulated by post-translational modifications to dictate isoform-specific functional differences (Bemben et al., 2014, 2015b; Jeong et al., 2017, 2019). Unlike other NLGNs, NLGN3 is localized to both excitatory and inhibitory synapses (Budreck and Scheiffele, 2007), but the molecular and functional segregation of NLGN3 on distinct synapses has not been fully understood. Importantly, the NLGN3 gene is localized to the X chromosome, and several missense or nonsense variants on *NLGN3* result in deficient glycosylation, folding, and trafficking of NLGN3. Thus, there is a strong association of NLGN3 with neuronal development and NLGN3 variants, in part, account for the male prevalence in NLGN-dependent cases of autism spectrum disorders (Jeong et al., 2017; Vieira et al., 2021).

Cdk5 is a proline-directed serine/threonine kinase and has brain-specific activity because of association with neuronal regulatory proteins p35 or p39 (Tsai et al., 1994). Various pre- and post-synaptic proteins, such as WAVE1, CASK, TH, PSD-95, DARPP-32, dopamine, and NMDA receptor subunits (Bibb et al., 1999; Wang et al., 2003; Morabito et al., 2004; Moy and Tsai, 2004; Kim et al., 2006; Samuels et al., 2007; Zhang et al., 2008; Jeong et al., 2013), have been identified as Cdk5 substrates. The Cdk5/p35 complex destabilizes the β-catenin-N-cadherin association and promotes cell migration (Kwon et al., 2000). $\alpha_1\beta_1$ integrin-induced activation of Cdk5 also triggers human neurofilament protein H (hNF-H) tail domain phosphorylation and promotes neurite outgrowth (Li et al., 2000). More recently, Cdk5 activity also has been implicated in neuronal transmission, synapse formation, and plasticity (Dhavan and Tsai, 2001). In neurotoxic conditions, proteolytic cleavage of p35 to p25 dysregulates Cdk5 activity, which affects tau phosphorylation and β-amyloid (Aβ) peptide accumulation that are associated with the pathology of neurodegenerative diseases (Baumann et al., 1993; Patrick et al., 1999; Cruz and Tsai, 2004).

Here, we characterized NLGN3 as a Cdk5 substrate for the first time. We find that NLGN3 is phosphorylated on S725. Until now, phosphorylation-mediated molecular mechanisms that are involved in the regulation of NLGN3 have not been actively investigated. Using mass spectrometry with our knock-in (KI) HA-tagged mouse, we find that Cdk5 is associated with NLGN3 *in vivo* throughout development. In addition, NLGN3 is directly phosphorylated by Cdk5 on S725. Using S725 mutations, we show that S725 phosphorylation affects NLGN3 interactions with Kalirin-7, NLGN3 surface expression, and synaptic transmission.

Materials and Methods

Plasmids and antibodies. pCAG-HA-NLGN3 WT (or S725A or S725D)-IRES-mCherry, pCAG-NLGN miRs-GFP, and pCMV-Cdk5/p35 plasmids were used for biochemical and imaging experiments. NLGN3 overexpression constructs were based on human NLGN3, and pCAG-NLGN miRs-GFP plasmids was characterized in a previous study (Shipman et al., 2011). Rat Cdk5 and p35 were subcloned into the pcDNA3.1/myc-His vector (Invitrogen). All point mutations were generated by PCR-based mutagenesis (QuickChange Site-Directed Instruction Manual). To generate the phosphorylation state-specific antibodies (pS733 NLGN1, pS714 NLGN2, or pS725 NLGN3-Ab), the synthetic phosphopeptides of each NLGN isoform were immunized to rabbits by New England Peptide. Sera were collected and affinity purified with an antigen phosphopeptide. The commercial antibodies used in this study were mouse anti-NLGN3 (Synaptic Systems, 129-113), rabbit anti-GST (Bethyl Laboratories), mouse anti-myc (Cell Signaling, clone 9B11), rabbit anti-HA (Abcam, ab9110), rat anti-HA (Roche), rabbit anti-Cdk5 (Santa Cruz Biotechnology, C-8), rabbit anti-β tubulin (Sigma, T2200), and mouse anti-β actin (ABM, G043).

HA-NLGN3 KI mouse generation. The HA-NLGN3 KI mouse line was generated with help from the Genetic Engineering Core of the National Eye Institute (Lijin Dong). An influenza hemagglutinin (HA) tag was inserted between the sequences encoding the signal peptide and the mature N-terminus of mouse Nlgn3 by CRISPR design. *Nlgn3* gRNA sequence: 5′GCT AAT ACG ACT CAC TAT AGG GGG CCA GTA CCC AGG CCC GTT TTA GAG CTA GAA. Oligo sequence for HA-Nlgn3: 5′-ATT GGT CCA CAG GAC CCA GGA TTT CAC TGG GCA ATG GTA CTC TGG CAC CCC TTA GCT TCC CAA AGT GAG TAT TGA CTG TGG GTG CCG GGG CCT GAG CGT AAT CTG GAA CAT CGT ATG GGT AGG TAC TGG CCC TCA GCA CCA AAC TGA GGA AGC. Primers for genotyping: 5′-CTG CCT ATT GGG CTG ATG CTG TGA and 5′-TGT GTG GCG TTC CGG ATG CCC GAC CA.

GST fusion protein production. Cytoplasmic regions of NLGNs were subcloned into the pGEX-4T plasmid and transformed to BL21 bacterial cells. Bacterial cultures were grown at 37°C to an absorbance at 600 nm of 1.1-1.2 of the culture media; 50 μM isopropyl β-d-1-thiogalactopyranoside was added to the cultures and incubated at 16°C overnight to induce fusion protein expression. The bacterial pellets were then lysed in a TBS buffer containing protease inhibitors (Roche), 100 μg/ml lysozyme, 15 mM DTT, 10 mM EDTA, and 1.5% Sarkosyl. The sonicated lysate was neutralized with Triton X-100 to a final concentration of 4%. The lysates were incubated with glutathione–Sepharose 4B (GE Healthcare) for 1 h at 4°C and subsequently washed with TBS buffer containing 1 mM EDTA and 0.1% Triton X-100.

In vitro *kinase assay.* GST fusion proteins were phosphorylated in 10 mM HEPES, pH 7.0, 20 mM $MgCl_2$, 50 μM ATP, and 1 pmol of [γ-^{32}P] ATP (3000 Ci mmol^{-1}) with 50 ng of purified active Cdk5 (Promega). *In vitro* kinase assays were performed at 30°C for 30 min. Proteins were eluted from the glutathione-Sepharose resin and resolved by SDS-PAGE and analyzed by immunoblotting.

Transfection and immunoblot. HEK293 cells were transfected with Lipofectamine 2000; and 2 d after transfection, the cells were lysed in a TBS buffer containing 150 mM NaCl, 50 mM Tris-HCl, pH 8.0, 1 mM EDTA, 1% Triton X-100. Lysates were centrifuged at 16,000 × *g* for 15 min at 4°C, and supernatants were used for the analysis. For coimmunoprecipitation, lysates were incubated with an appropriate antibody at 4°C overnight and protein-A-Sepharose beads (GE Healthcare) at 4°C for 1 h. Cultured cortical neurons were transfected at DIV 5 using calcium phosphate method as described previously (Won et al., 2016). The neurons were further lysed and fractionated for desired experiments. All chemiluminescence blots were captured with a ChemiDoc Imaging System (Bio-Rad).

Neuronal cultures. For biochemical analyses and immunocytochemistry experiments, we used primary cultured cortical and hippocampal neurons from embryonic day 18 (E18) Sprague Dawley rats of either sex. Briefly, embryonic hippocampal or cortical tissues were dissociated at 37°C for 30 min by 0.05% trypsin in 10 mM HBSS containing 1.37 mg/ml DNase I. Neurons were plated and maintained in serum-free Neurobasal Medium supplemented with 2% (v/v) B-27 and 2 mM L-glutamine. We adhered to the guidelines of the National Institutes of Health's Animal Care and Use Committee regarding the care and use of animals for this study (Protocol #1171).

Subcellular fractionation of brain tissue. Biochemical fractionation was conducted as described in our previous studies (Sanz-Clemente et al., 2010; Bemben et al., 2014; Won et al., 2016). Briefly, mouse of either sex or female rat brain tissue were homogenized in ice-cold TEVP buffer (320 mM sucrose, 10 mM Tris-HCl, pH 7.5, 5 mM EDTA, 1 × protease inhibitor mixture (Roche, 11697498001), and phosphatase inhibitor

mixture II (Sigma, P5726) and III (Sigma, P0044)). Homogenates (H) were centrifuged at 1000 × *g* for 10 min at 4°C. The supernatant (S1) was centrifuged at 10,000 × *g* for 20 min at 4°C to get P2 pellet (crude synaptosomal fraction). The P2 pellet was lysed in an appropriate buffer for analysis.

Surface biotinylation. Cultured cortical neurons at DIV 17-20 were washed 3 times with cold PBS (including 2 mM $CaCl_2$ and 1 mM $MgCl_2$). Neurons were incubated with 1 mg/ml biotin (EZLink Sulfo-NHS-LC-Biotin, Fisher Scientific, #21335) in PBS (including 2 mM $CaCl_2$ and 1 mM $MgCl_2$) for 30 min at 4°C and subsequently quenched free biotin by incubating neurons with PBS containing 100 mM glycine for 20 min. After washing, neurons were lysed with RIPA buffer (150 mM NaCl, 50 mM Tris-HCl, pH 7.8, 1 mM EDTA, 1% Triton X-100, 0.5% deoxycholic acid, 0.5% SDS). The lysates were vigorously sonicated, and supernatants were incubated with NeutrAvidin agarose resin (Fisher Scientific, #29202) for 1-2 h. Proteins were eluted from the agarose resin and resolved by SDS-PAGE, and analyzed by immunoblotting.

Immunocytochemistry. Cultured hippocampal neurons were grown on glass coverslips precoated with poly-D-lysine (Sigma). Neurons were cotransfected with pCAG-NLGN miRs-GFP and pCAG-HA-NLGN3 (WT, S725A, or S725D) plasmids with Lipofectamine 2000 at DIV 12-15 and prepared for analysis at DIV 19-21. To label surface HA-NLGN3, transfected neurons were labeled with rat anti-HA antibody for 15 min at room temperature. Neurons were washed with PBS and fixed with 4% PFA and 4% sucrose in PBS for 10 min. The cells were incubated with Alexa 555-conjugated anti-rat secondary antibody (Invitrogen). After surface labeling, the neurons were permeabilized with 0.25% Triton X-100 in PBS and blocked with 10% goat serum. Intracellular HA-NLGN3 was labeled with rabbit anti-HA antibody and Alexa 647-conjugated anti-rabbit secondary antibody. For analysis, regions from three dendrites per each neuron were collected and quantified by the fluorescence intensity of target proteins. All images were captured with a 63× objective on a Zeiss LSM 510 confocal microscope and analyzed with the ImageJ and MetaMorph version 7.

Mass spectrometry. For phosphorylation site mapping, ~ 1 µg in-gel samples were alkylated with N-ethylmaleimide and digested with chymotrypsin at 25°C for 18 h. Peptides were extracted then desalted before being injected into a nano-LC/MS/MS system where an Ultimate 3000 HPLC was coupled to an Orbitrap Lumos mass spectrometer (Fisher Scientific) via an Easy-Spray ion source (Fisher Scientific). Peptides were separated on a ES802 Easy-Spray column (75 µm inner diameter, 25 cm length, 3 µm C18 beads; Fisher Scientific) with a 38 min linear gradient of 5%-24% mobile phase B (mobile phase A: 0.1% formic acid in LC-MS grade water; mobile phase B: 0.1% formic acid in LC-MS grade acetonitrile) at a flow rate of 300 nl/min. Thermo Scientific Orbitrap Lumos mass spectrometer was operated in data-dependent mode. The resolution of the survey scan was set at 120,000 at m/z 400. The m/z range for MS scans was 350-1500. For MS/MS data acquisition, the ETciD method was used, the minimum signal intensity required to trigger MS/MS scan was 5e3, the isolation width was 2.0 m/z, and the dynamic exclusion window was 6 s. MS1 scan was performed every 3 s. As many MS2 scans were acquired within the MS1 scan cycle. Xcalibur RAW files were converted to peak list files in mgf format using Mascot Distiller. Database search was performed using Mascot Daemon (2.5.0) against Sprot Mouse database. Mass tolerances for MS1 and MS2 scans were set to 5 ppm and 0.3 Da, respectively. Oxidation (M) and phosphorylation (STY) were searched as variable modification. Spectra of phosphopeptides matched by database search were manually checked.

The samples for label-free quantitation analysis were treated differently. The differences are summarized below; ~10 µg in-gel samples were alkylated with N-ethylmaleimide and digested with trypsin at 37°C for 18 h. Peptides were separated on a ES802 column with mobile phase B increased from 5% to 24% in 92 min. CID fragmentation method was used for MS2 scans. The dynamic exclusion window was 12 s. Proteome Discoverer software version 2.4 was used for protein identification and quantitation. Raw data were searched against Sprot Mouse database. Mass tolerances for MS1 and MS2 scans were set to 5 ppm and 0.6 Da, respectively. The search results were filtered by a false discovery rate of 1% at the protein level. For each sample, protein abundance values were calculated for all proteins identified by summing the abundance of unique peptides matched to that protein. The ratios were calculated using protein abundance method without normalization. Individual protein ANOVA method was used for hypothesis test.

Electrophysiological recording. The mEPSC and mIPSC recordings were performed in dissociated rat hippocampal primary cultures (DIV 15-17). Recordings were done in ACSF containing 119 mM NaCl, 2.5 mM KCl, 26 mM $NaHCO_3$, 1 mM Na_2PO_4, 11 mM glucose, 2.5 mM $CaCl_2$, and 1.3 mM $MgCl_2$; 0.1 mM picrotoxin (mEPSCs) or 20 µm DNQX (mIPSCs), and 0.5 µM TTX were added to the ACSF before recording. The intracellular solution for mEPSC recording contained the following (in mM): 135 $CsMeSO_4$, 8 NaCl, 10 HEPES, 0.3 Na_3GTP, 4 MgATP, 0.3 EGTA, 5 QX-314, and 0.1 spermine. The intracellular solution for mIPSCs recording contained the following (in mM): 70 $CsMeSO_4$, 70 CsCl, 8 NaCl, 10 HEPES, 0.3 NaGTP, 4 Mg_2ATP, and 0.3 EGTA, adjusted to pH 7.3 with CsOH. The osmolality of the solutions was adjusted from 285 to 290 mOsm, and pH was buffered from 7.25 to 7.35. The mEPSCs and mIPSCs were recorded at −70 mV, and the analysis of the mEPSCs was done semi-automatically, using in-house software Igor Pro (Wavemetrics) developed in Roger Nicoll's laboratory at the University of California–San Francisco. All events were visually inspected to ensure they were mEPSCs or mIPSCs during analysis, and those noncurrent traces were discarded. Series resistance was monitored and not compensated, and cells in which series resistance varied by 25% during a recording session were discarded. Synaptic responses were collected with a Multiclamp 700B amplifier (Molecular Devices), filtered at 2 kHz, and digitized at 10 kHz. All pharmacological reagents were purchased from Abcam, and other chemicals were purchased from Sigma.

Statistical analysis. Data analysis was conducted in Image Lab Software (Bio-Rad) or GraphPad Prism (GraphPad Software). Student's *t* test and one-way ANOVA with Dunnett's multiple comparison test were used for the analysis of biochemical and immunocytochemical data. For all statistical analysis, $p < 0.05$ was considered significant, and data are presented as mean ± SEM.

Results

NLGN3 S725 is phosphorylated *in vivo*

NLGNs display isoform-dependent effects on synaptic transmission and plasticity. We know that isoform-specific regulation by post-translational mechanisms, such as phosphorylation, is important for synaptic effects (Bemben et al., 2015a; Jeong et al., 2017) (Fig. 1*A*). NLGN1 T739, 15 amino acids downstream of the transmembrane domain, was identified as a CaMKII phosphorylation site, and the phosphorylation is required for efficient NLGN1 surface expression (Bemben et al., 2014). In addition, isoform-specific PKC phosphorylation on NLGN4X T707 increases spine formation and glutamate receptor currents. Notably, a nearby autism mutation (R704C) eliminates PKC phosphorylation of NLGN4X T707 (Bemben et al., 2015b).

To facilitate isolation and characterization of NLGN3, we introduced an epitope tag. Specifically, we generated an HA-NLGN3 KI mouse to investigate phosphorylation of NLGN3 *in vivo*. CRISPR KI was designed to insert the HA epitope in the extracellular domain of NLGN3 (Fig. 1*B*, left). Genomic modification for HA-tagging was confirmed by genotyping PCR (Fig. 1*B*, middle). To evaluate the HA-tagged protein *in vivo*, we collected P2 pellets from WT and the KI mouse brains and proteins were analyzed by immunoblotting. We confirmed the HA epitope recognition for NLGN3 in KI mice (Fig. 1*B*, right). To identify *in vivo* phosphorylation of NLGN3, we enriched HA-NLGN3 by immunoprecipitation from P2 pellet lysates of the KI mouse brains at different developmental stages (P6, P12, P18, P21, and P35) and LC-MS/MS was performed (Fig. 1*C*, left). We found that NLGN3 was phosphorylated on S725 (S722 in mouse NLGN3,

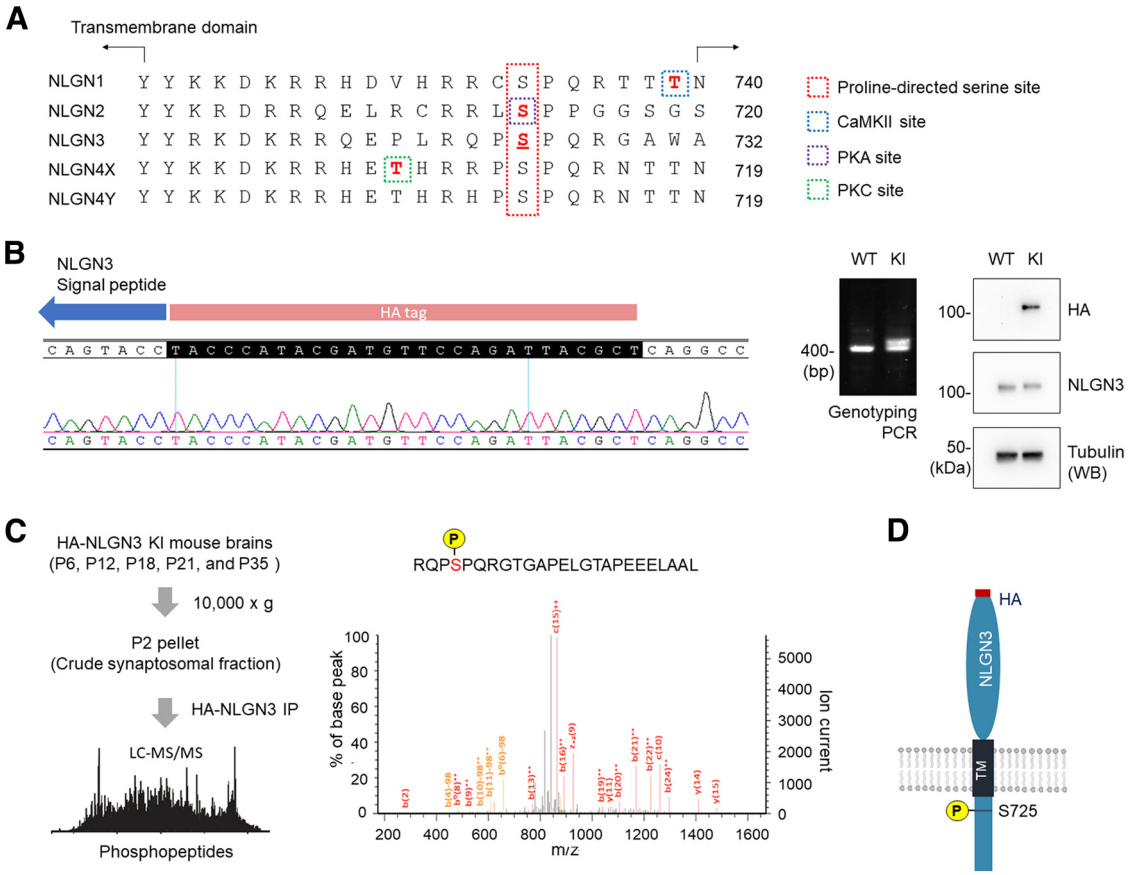

Figure 1. NLGN3 S725 is phosphorylated *in vivo*. ***A***, Sequence alignment for the juxta-membrane region of the NLGN isoform C-tails. ***B***, HA-tag insertion was confirmed by Sanger sequencing of PCR product from gDNA of the mouse line (left). Middle, Genotyping for HA-NLGN3 KI mice. Right, Immunoblot analysis of HA-NLGN3 from the mouse brain P2 lysates. ***C***, Schematic diagram of the identification of *in vivo* NLGN3 phosphorylation (left). Mouse brains from different developmental stages were isolated and the P2 pellets were prepared. HA-NLGN3 was enriched by immunoprecipitation using HA-antibody and analyzed by LC-MS/MS. MS/MS spectrum of the endogenous NLGN3 S725 phosphorylated peptide (right). ***D***, Schematic represents HA-tagging and S725 phosphorylation site on NLGN3.

but we will use the numbering of the human sequence for consistency between the human NLGN3 cDNA plasmids and our mouse studies) in all prepared samples, which indicates that NLGN3 phosphorylation on S725 is present throughout brain development (Fig. 1*C*, right). All these data show *in vivo* phosphorylation of NLGN3 S725 and suggest a physiological role of NLGN3 phosphorylation on S725 during neuronal development (Fig. 1*D*).

Cdk5 phosphorylates NLGN3 on S725

To identify kinases that phosphorylate NLGN3, we prepared P2 pellet lysates and LC-MS/MS was performed as described previously (Fig. 2*A*). We screened for interacting kinases with adequate enrichment relative to control. The enrichment abundancy (Log_2 fold change) and significance ($-Log_{10}$ P value) were analyzed (Fig. 2*A*). We identified a number of kinases as NLGN3 interacting proteins, including CaMKV and GSK3β, that play various roles in brain development, including axon guidance, spine formation, and neurotransmitter release (Fig. 2*A*; Extended Data Table 2-1). We were particularly intrigued with Cdk5, which was highly associated with NLGN3 in all our samples from different developmental stages (Fig. 2*A*). NLGN3 S725 is located within a Cdk5 consensus sequence, (S/T)-P-X-(K/H/R) (Dhavan and Tsai, 2001), and close to the transmembrane region of NLGN3 (Fig. 1*A*). p35, a Cdk5 activator, was not found in our mass spectrometry analysis (Extended Data Table 2-1). Although active Cdk5/p35 complex is targeted to plasma membrane by myristoylation (Dhavan and Tsai, 2001), Cdk5 targeting NLGN3 near the transmembrane region is consistent. We raised a phosphorylation state-specific antibody against pS725 to characterize the phosphorylation of NLGN3 S725 further. Phosphorylated NLGN3 was immunoprecipitated using the pS725 antibody from rat brain P2 pellets. The immunoprecipitates were analyzed by immunoblotting, and endogenous NLGN3 and Cdk5 were both enriched (Fig. 2*B*).

To determine whether Cdk5 is able to phosphorylate NLGN3, GST-NLGN3 C-tail fusion proteins (WT and S725A) were incubated with purified Cdk5/p35 complex and [γ-^{32}P] ATP. When S725 is mutated to alanine, a phosphodeficient mutation, Cdk5 phosphorylation assessed by incorporation of radioactive ATP was dramatically decreased in an *in vitro* kinase assay (Fig. 2*C*), showing that S725 is a Cdk5 phosphorylation site. Histone was used as a positive control for Cdk5 phosphorylation. GST-NLGN3 WT fusion proteins were incubated with or without purified Cdk5/p35 complexes and ATP *in vitro*. Samples were resolved by SDS-PAGE and analyzed by immunoblotting with pS725 antibody. We observed Cdk5/p35-dependent immunoreactivity for GST-NLGN3 (Fig. 2*D*).

To determine whether full-length NLGN3 can be phosphorylated by Cdk5, we cotransfected HA-NLGN3 WT or HA-NLGN3 S725A and Cdk5/p35 plasmids in HEK293 cells. The cell lysates were analyzed by immunoblotting with pS725 antibody. The immunoblots showed increased immunoreactivity for NLGN3 WT on Cdk5/p35 cotransfection, which was not the case for the NLGN3 S725A (Fig. 2*E*). We also observed that a pharmacological

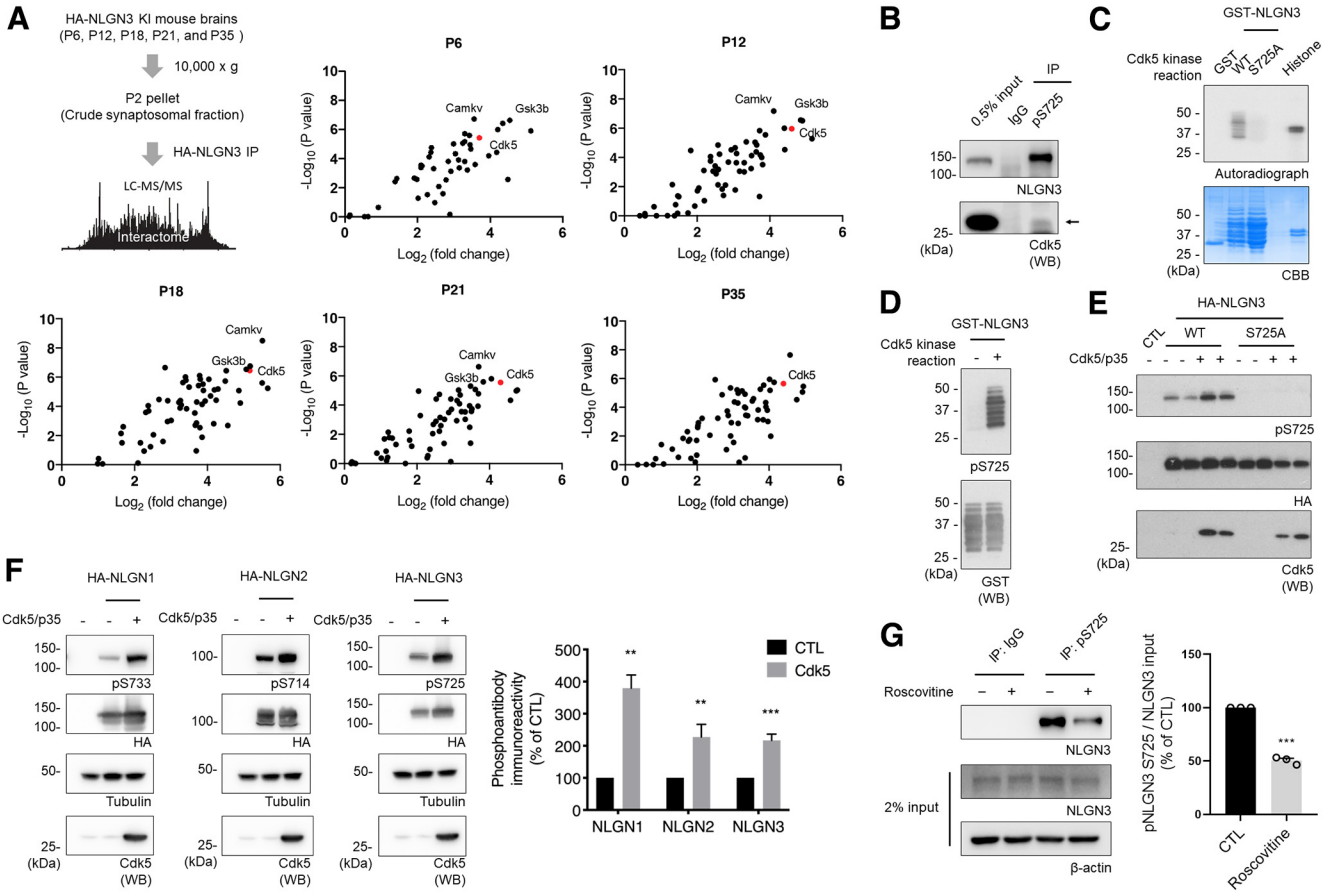

Figure 2. Cdk5 phosphorylates NLGN3 on S725. ***A***, HA-NLGN3 KI mouse brains were prepared as described previously. HA-NLGN3 was immunoprecipitated using HA-antibody, and the immunoprecipitates were analyzed by LC-MS/MS. Cdk5 is indicated on a volcano plot of kinases enriched in the immunoprecipitates (red). ***B***, Endogenous pS725 NLGN3 was enriched from WT mouse brain P2 lysates by immunoprecipitation using pS725 antibody with IgG as a negative IP control. Arrow indicates the Cdk5 position in the blot. ***C***, Autoradiography analysis of GST-NLGN3 WT and S725A fusion proteins that were incubated with purified Cdk5/p35 complex and [γ-^{32}P] ATP. ***D***, Immunoblot analysis of GST-NLGN3 fusion proteins that were phosphorylated *in vitro* with purified Cdk5/p35. ***E***, Immunoblot analysis of HA-NLGN3 WT and S725A transfected or cotransfected with Cdk5/p35 in HEK293 cells. ***F***, HA-NLGN1, HA-NLGN2, or HA-NLGN3 was transfected or cotransfected with Cdk5/p35 in HEK293 cells, and the cell lysates were analyzed by immunoblotting with NLGN3 S725 or analogous site phosphorylation state-specific antibodies. ***G***, Cultured cortical neurons were treated with 20 μM roscovitine, a Cdk5 inhibitor, and endogenous pS725 NLGN3 was enriched by immunoprecipitation using pS725 antibody. The ratio of immunoprecipitated pS725 NLGN3/NLGN3 input was analyzed. Graph represents mean ± SEM ($n = 3$). $^{**}p < 0.002$; $^{***}p < 0.0002$; unpaired *t* test. Data corresponding to this figure are included in Extended Data Table 2-1.

inhibition of Cdk5 reduced endogenous NLGN3 enrichment by immunoprecipitation using pS725 antibody from cultured neurons (Fig. 2*G*). All these results demonstrate that Cdk5 can phosphorylate NLGN3 on S725 in a cellular and neuronal context.

We also raised other phosphorylation state-specific antibodies against the analogous residue in other NLGN isoforms: pS733 (NLGN1) and pS714 (NLGN2). We used these antibodies to characterize the phosphorylation of NLGN1 and NLGN2 by cotransfecting HA-NLGN1, HA-NLGN2, or HA-NLGN3 and Cdk5/p35 plasmids in HEK293 cells. The cell lysates were analyzed by immunoblotting with NLGN1 pS733, NLGN2 pS714, or NLGN3 pS725 antibodies, and we observed increased phosphoantibody immunoreactivity for all NLGN isoforms on Cdk5/p35 cotransfection (Fig. 2*F*). These results indicate that Cdk5 is able to phosphorylate NLGN1 and NLGN2 on sites analogous to NLGN3 S725 *in situ*, supporting a conserved proline-directed serine consensus site, which could be a hot spot for Cdk5-dependent regulation of several isoforms of NLGNs.

NLGN3 S725 mutations affect the kalirin-7 interaction

Multiple papers have shown that the intracellular region of NLGNs is critical for protein binding and subsequent neuronal signaling pathways (Irie et al., 1997; Bemben et al., 2015a; Jeong et al., 2017). NLGN2 S714 phosphorylation recruits Pin1 to negatively regulate NLGN2/gephyrin binding (Antonelli et al., 2014), but none of the studies thus far has extensively tested the effect of NLGN3 S725 phosphorylation on other protein–protein interactions. We examined the NLGN3 S725 mutant (S725A or S725D) binding with PSD-95 or Gephyrin, which are well-known NGLN3 binding partners at excitatory or inhibitory synapses, respectively. We cotransfected HA-NLGN3 (WT, S725A, or S725D) and PSD-95-myc or myc-Gephyrin in HEK293 cells. HA-NLGN3 was immunoprecipitated, and any coimmunoprecipitated PSD-95-myc or myc-Gephyrin was analyzed by immunoblotting. For both cases, NLGN3 S725 mutants did not show any significant changes in binding with PSD-95-myc or myc-Gephyrin (Fig. 3*A*,*B*).

Recently, we found that the RhoGEF Kalirin-7 interacts with NLGN isoforms and mediates NLGN1 function in neurons (Paskus et al., 2019). Kalirins are essential RhoGEFs, regulating spine dynamics and synaptic plasticity (Penzes and Jones, 2008; Herring and Nicoll, 2016). We examined whether NLGN3 S725 phosphorylation affects Kalirin binding with NLGN3. Using the same approach as above, we cotransfected HA-NLGN3 (WT, S725A, or S725D) and myc-Kalirin-7 in HEK293 cells. The cells

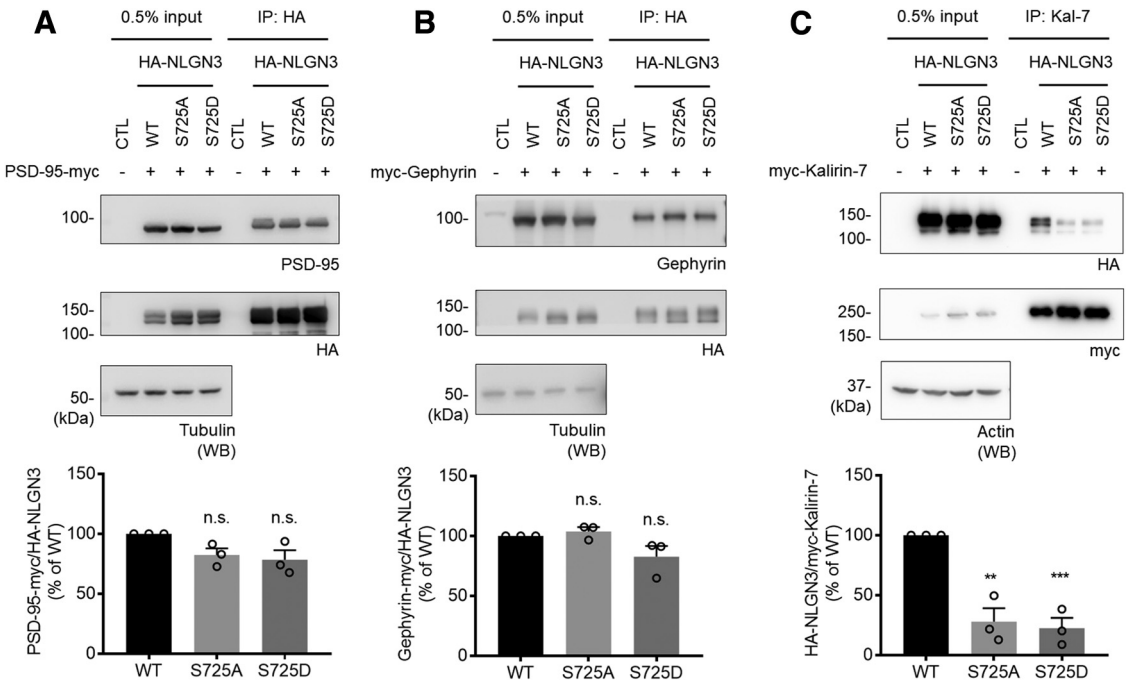

Figure 3. NLGN3 S725 mutations affect the Kalirin-7 interaction. HEK293 cells were cotransfected with plasmids as indicated in the figures. ***A***, ***B***, Coimmunoprecipitated PSD-95-myc or myc-Gephyrin were analyzed by immunoblotting (with HA antibodies). The ratio of coimmunoprecipitated PSD-95-myc or myc-Gephyrin/immunoprecipitated HA-NLGN3 was analyzed. ***C***, HA-NLGN3 in the immunoprecipitates with Kalirin-7 antibody were analyzed by immunoblotting. The ratio of coimmunoprecipitated HA-NLGN3/immunoprecipitated myc-Kalirin-7 was analyzed. Graph represents mean ± SEM ($n = 3$-5). The statistical significance between the mean of WT and the mean of each condition was calculated using one-way ANOVA with Dunnett's multiple comparison test. $^{**}p = 0.0013$; $^{***}p = 0.0009$; *post hoc* tests.

were lysed, myc-Kalirin-7 was immunoprecipitated, resolved by SDS-PAGE, and coimmunoprecipitated HA-NLGN3 was analyzed by immunoblotting. Interestingly, HA-NLGN3 S725A and S725D showed significantly decreased binding to myc-Kalirin-7 compared with NLGN3 WT (Fig. 3*C*).

Our results indicate that NLGN3 S725 phosphorylation does not affect the NLGN3 interactions with postsynaptic scaffolding proteins, such as PSD-95 and Gephyrin. Meanwhile, both NLGN3 S725A and S725D disrupt the dynamic phosphorylation on S725 and reduce the NLGN3 interaction with Kalirin-7. This indicates that NLGN3 S725 phosphorylation is important for the Kalirin-7 interaction and NLGN3 S725A and S725D are indistinguishable for the Kalirin-7 binding.

NLGN3 S725 mutations modulate NLGN3 surface expression in cultured neurons

To determine any direct effects of S725 phosphorylation on NLGN3 localization and function, we examined the surface levels of NLGN3 WT or S725 phospho-mutant in cultured rat hippocampal neurons. We cotransfected cultured hippocampal neurons with HA-NLGN3 (WT, S725A, or S725D) and NLGN miRs to knock down endogenous NLGNs and allow precise evaluation of expressed WT and mutant proteins. Surface and intracellular HA-NLGN3 was labeled at DIV 20-22, and the dendritic regions were imaged for analysis. Notably, both the NLGN3 S725A and S725D mutations increased surface expression of NLGN3 (Fig. 4*A*,*B*) relative to WT, indicating that the intact phosphorylation on NLGN3 S725 is required for proper NLGN3 surface expression in cultured neurons.

NLGN3 phosphorylation by Cdk5 is implicated in spine formation and NLGN3 trafficking

We further analyzed spine numbers of the hippocampal neurons cotransfected with HA-NLGN3 (WT, S725A, or S725D) and NLGN miRs. NLGN3 S725A and S725D did not change the total spine numbers in mature cultured neurons (DIV 15-22) (Fig. 4*B*). We also saw NLGN3 S725A and S725D nearly rescue the total spine numbers in immature cultured neurons (DIV 10-12), although S725D did to a lesser extent to NLGN3 WT (Fig. 5*A*,*B*). These data indicate that S725 phosphorylation has a limited effect on the spine formation.

Interestingly, when we analyzed endogenous NLGN3 surface expression in cultured neurons treated with a Cdk5 inhibitor, surface expression of endogenous NLGN3 was reduced on the pharmacological inhibition of Cdk5 activity (Fig. 5*C*). We also observed reduced surface expression of transferrin receptor, which indicates that NLGN3 surface expression is under control of a broad regulation of neuronal membrane protein trafficking by Cdk5 activity.

NLGN3 S725 is important for excitatory and inhibitory synaptic transmission

To investigate further the effects of S725 phosphorylation on synaptic transmission, we measured AMPAR mEPSCs in hippocampal cultured neurons expressing either NLGN miRs alone or NLGN miRs and HA-NLGN3 (WT, S725A, or S725D) at DIV 15-17 (Fig. 6*A*,*B*). Knockdown of endogenous NLGNs reduced both mEPSC frequency and amplitude (Fig. 6*C*,*D*). HA-NLGN3 S725 rescued the reduced mEPSC frequency, while both HA-NLGN3 S725A and S725D further increased mEPSC frequency compared with WT (Fig. 6*C*). HA-NLGN3 WT also rescued the reduced mEPSC amplitude, and both HA-NLGN3 S725A and S725D restored the impaired EPSC amplitude similar extent to NLGN3 WT (Fig. 6*D*).

To examine the functional significance of S725 phosphorylation on inhibitory synaptic transmission, we measured mIPSCs (Fig. 7*A*,*B*). Neurons transfected with NLGN miRs, compared with the negative control group, showed a significant reduction

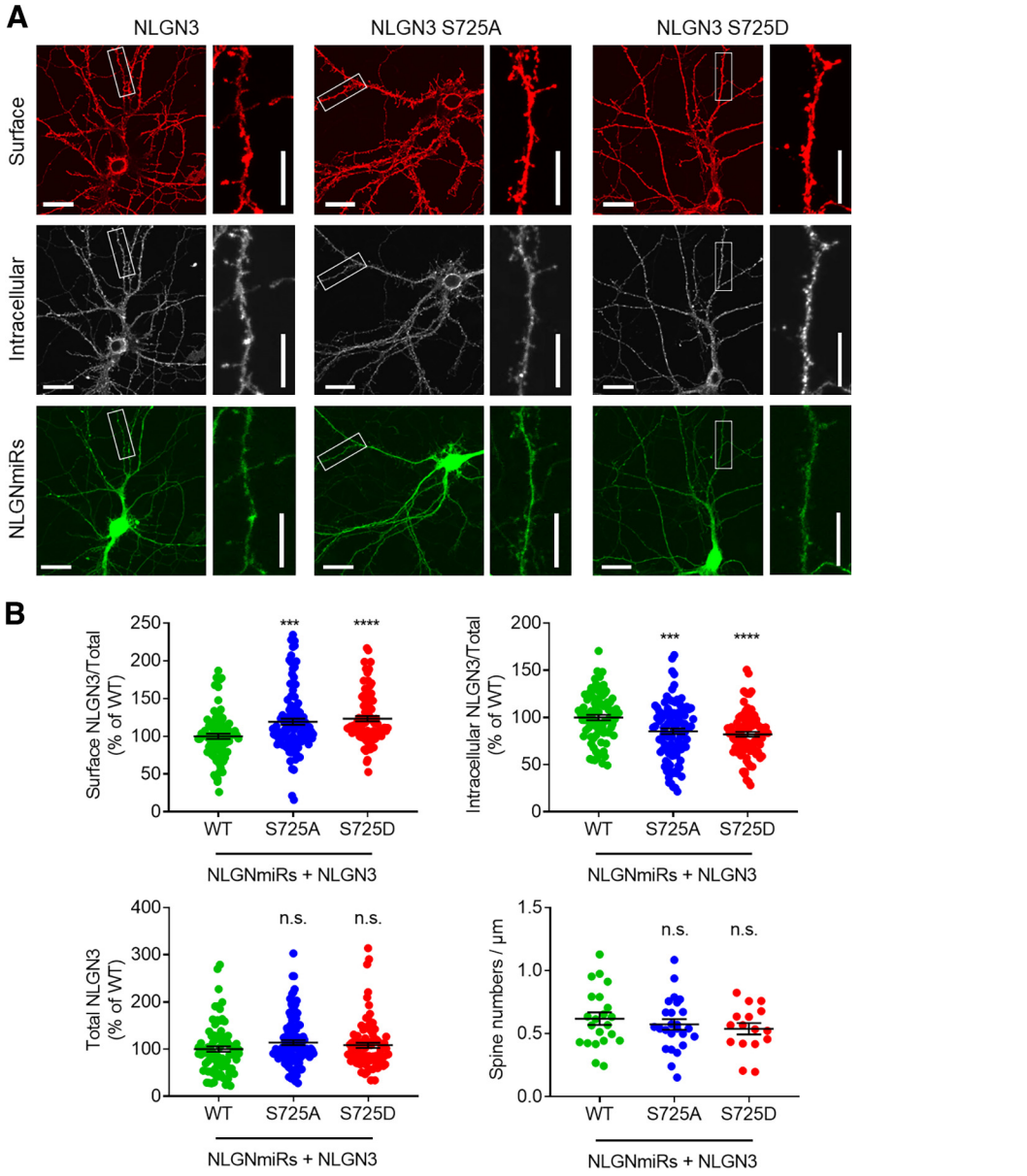

Figure 4. NLGN3 S725 mutations modulate NLGN3 surface expression in cultured neurons. ***A***, NLGN miRs (green) and HA-NLGN3 (WT, S725A, or S725D) were coexpressed in cultured hippocampal neurons (DIV 15-22). Enlarged images of the boxed regions are shown below each panel. Surface HA-NLGN3 was labeled with anti-HA and Alexa 555-conjugated secondary antibody (red). After fixation and permeabilization, intracellular HA-NLGN3 was stained with anti-HA and Alexa 647-conjugated secondary antibody (white). Scale bars: high magnification, 25 μm; low magnification, 50 μm. ***B***, Regions from three dendrites per neuron were collected for analysis. HA-NLGN3 S725A and S725D were normalized to HA-NLGN3 WT. Graph represents mean ± SEM. The statistical significance between the mean of WT and the mean of each condition was calculated using one-way ANOVA with Dunnett's multiple comparison test. p values for one-way ANOVA < 0.0001. ***$p < 0.001$; ****$p < 0.0001$; *post hoc* tests (Surface NLGN3/Total and Intracellular NLGN3/Total).

in both mIPSC frequency and amplitude. And the mIPSC frequency and amplitude reductions were fully reversed when HA-NLGN3 was introduced. We observed that both HA-NLGN3 S725A and S725D mutants led to a significant decrease in mIPSC frequency compared with WT, while the mIPSC amplitudes remained unchanged (Fig. 7*C*,*D*). Interestingly, despite the increased surface expression levels of NLGN3 S725 mutants that we observed (Fig. 4), the reduction in mIPSC frequency induced by NLGN miRs was not restored by either NLGN3 S725A or S725D. This suggests that these two mutants may affect the function of NLGN3 at inhibitory synapses. Furthermore, our findings indicate that the NLGN3 S725A and S725D mutations did not disrupt the interaction of NLGN3 with postsynaptic scaffolding proteins (Fig. 3) and did not alter the mIPSC amplitude (Fig. 7*D*). Thus, the observed effects are unlikely to be caused by remodeling of the postsynaptic protein complex. Further molecular investigations are required to elucidate the detailed regulatory mechanisms underlying these findings.

Discussion

There are two conserved serine sites in the cytosolic region of NLGNs: one is adjacent to the PDZ ligand at the cytosolic tail and the other is 15 amino acids downstream of the transmembrane domain. The former serine site on NLGN1 (S839) is phosphorylated by PKA, and the phosphorylation modulates NLGN1

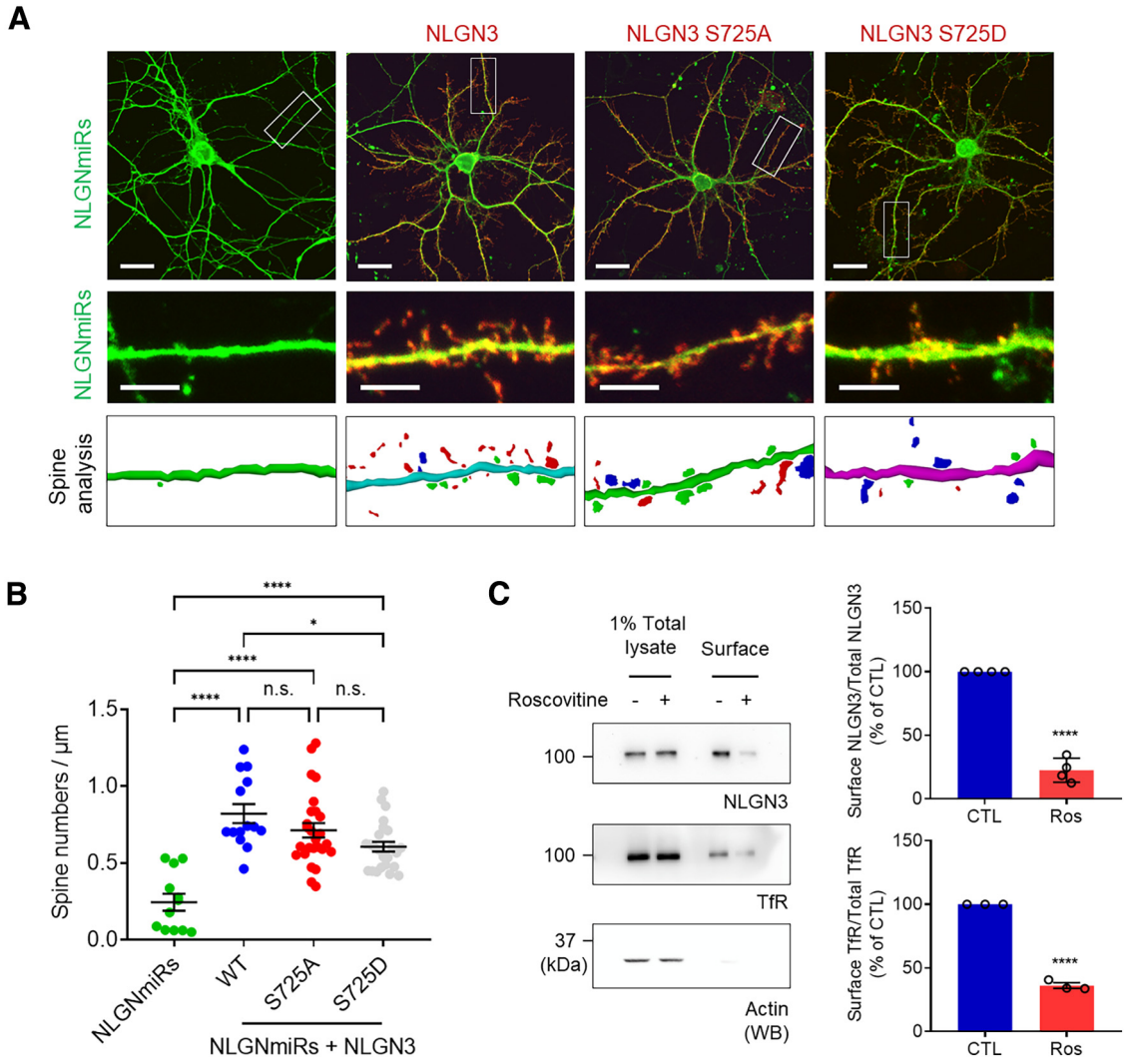

Figure 5. NLGN3 phosphorylation by Cdk5 is implicated in spine formation and NLGN3 trafficking. ***A***, NLGN miRs (green) and HA-NLGN3 (WT, S725A, or S725D) were coexpressed in cultured hippocampal neurons (DIV 10-12). Enlarged images of the boxed regions are shown below each panel. Surface HA-NLGN3 was labeled with anti-HA and Alexa 555-conjugated secondary antibody (red). Scale bars: high magnification, 25 μm; low magnification, 50 μm. ***B***, Regions from three dendrites per neuron were collected for analysis. Graph represents mean ± SEM. The statistical significance between the mean of WT and the mean of each condition was calculated using one-way ANOVA with Dunnett's multiple comparison test. p values for one-way ANOVA $<$ 0.000001. *$p < 0.05$; ****$p < 0.0001$; *post hoc* tests. ***C***, Cultured cortical neurons were treated with 20 μM roscovitine, a Cdk5 inhibitor, and surface biotinylation assays were performed as described in Materials and Methods. Graph represents mean ± SEM ($n = 3$). ****$p < 0.0001$ (unpaired t test).

surface levels and PSD-95 binding (Jeong et al., 2019). The latter conserved serine site on NLGN2, S714, undergoes proline-directed phosphorylation and the phosphorylation recruits Pin1 to negatively regulate NLGN2/gephyrin binding (Antonelli et al., 2014). Recently, Halff et al. (2022) showed that PKA phosphorylates NLGN2 S714, and the phosphorylation disperses NLGN2 from the synapse and reduces NLGN2 surface expression, leading to a loss of synaptic $GABA_A$Rs. Here we characterized NLGN3 S725, the conserved serine residue in NLGN3 that is analogous to NLGN2 S714, as a novel Cdk5 phosphorylation site, which regulates NLGN3 surface expression and excitatory synaptic transmission.

Using a proteomic analysis of the brain samples, we identified a number of NLGN3 interacting kinases other than Cdk5, such as CaMKV and GSK3β. These interactions were detected at different developmental stages (Fig. 2*A*). These kinases have been known to play various roles in brain development, including axon guidance, spine formation, and neurotransmitter release (Dhavan and Tsai, 2001; Hur and Zhou, 2010; Liang et al., 2016). Our findings suggest that NLGN3 S725 could be phosphorylated by a variety of kinases with cellular consequences throughout brain development. As Halff et al. (2022) showed, most of NLGN2 is basally phosphorylated in cultured neurons. Our study also revealed the conserved proline-directed serine sites in NLGN1, NLGN2, and NLGN3 can be phosphorylated in the basal state in cell lines (Fig. 2*F*). These findings indicate that the basal phosphorylation of the conserved proline-directed serine residues in NLGNs might be important for intrinsic NLGN features. The signaling pathway that modulates Cdk5-mediated NLGN3 S725 phosphorylation has not been fully investigated in our current study. Intensive molecular studies will be required to understand the dynamic regulation of the phosphorylation by the kinases following neuronal activity or temporal developmental cues.

In the current study, we found that NLGN3 S725 phosphorylation does not affect the NLGN3 interaction with postsynaptic scaffolding proteins, such as PSD-95 and gephyrin (Fig. 3*A*,*B*). It could be the result of the physical distance between the S725 site

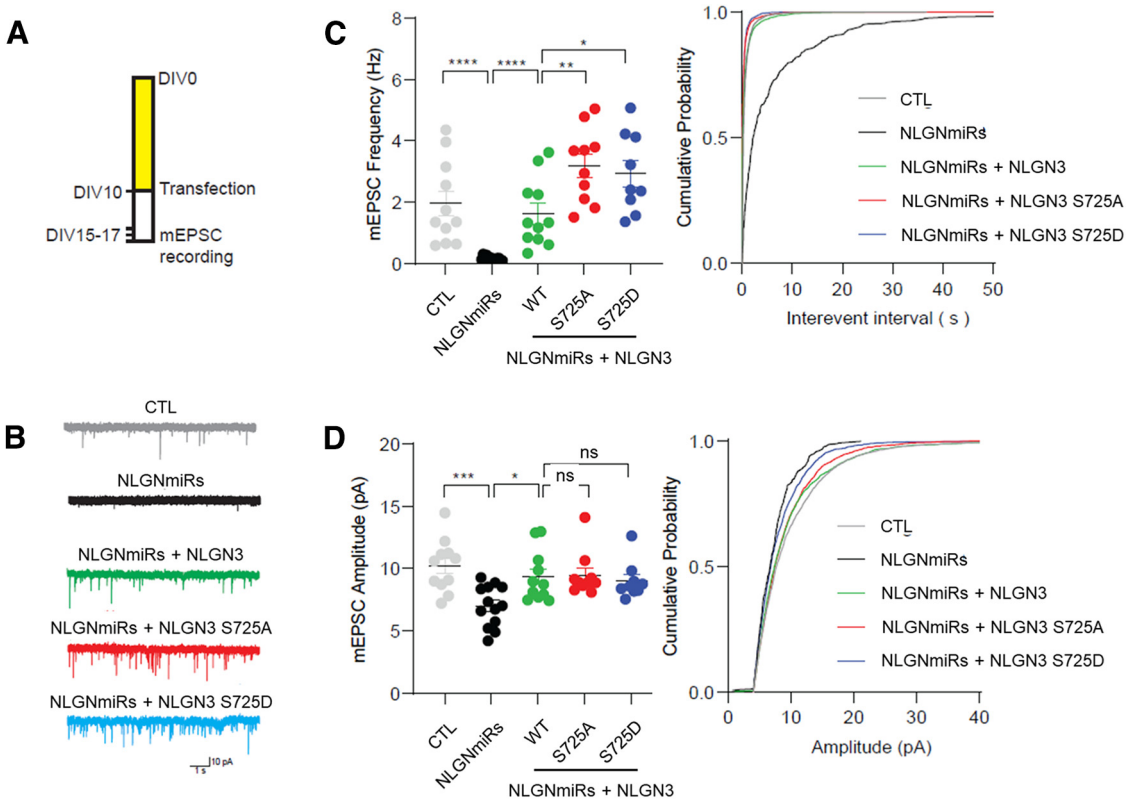

Figure 6. NLGN3 S725 is important for excitatory synaptic transmission. ***A***, Cultured hippocampal neurons were transfected at DIV 10, and mEPSC recording was performed at DIV 15-17. ***B***, Representative AMPAR mEPSC traces recorded in cultured hippocampal neurons expressing either NLGN miRs or NLGN miRs and HA-NLGN3 (WT, S725A, or S725D). ***C***, Spontaneous AMPAR mEPSC mean frequency and cumulative probability. $*p < 0.05$. $**p < 0.025$. $****p < 0.0001$. ***D***, Spontaneous AMPAR mEPSC mean amplitude and cumulative probability. $*p < 0.05$. $***p < 0.001$. The statistical significance between every condition was calculated using one-way ANOVA with Brown-Forsythe and Welch test for multiple comparison.

and the binding motifs for the scaffolding proteins. Instead, intriguingly, we found that both the NLGN3 S725A and S725D mutations significantly inhibit the NLGN3 interaction with Kalirin-7 (Fig. 3*C*). Kalirin-7 is the brain-specific neuronal guanine nucleotide exchange factor (GEF), which activates the small GTPase Rac1 (Penzes et al., 2000; Penzes and Jones, 2008). Rac1 is a positive modulator for spine formation and enlargement (Tashiro et al., 2000; Xie et al., 2007). In our previous study, we found that Kalirin-7 interacts with NLGN1 and mediates NLGN1-dependent synaptic functions (Paskus et al., 2019). Together, these findings support the conclusion that NLGN3 S725 phosphorylation is not intimately involved in postsynaptic scaffolding protein-mediated synaptic regulations, but rather it is associated with the Kalirin-7-mediated regulation of spine development. Kalirin-7 retains the PDZ interaction motif that targets Kalirin-7 to synapse, suggesting a role of Kalirin-7 to regulate dendritic morphology and synapse formation. Since we observed that NLGN3 S725A and S725D reduce Kalirin-7 binding (Fig. 3*C*) and increase NLGN3 surface expression (Fig. 4*A*), we can estimate that Kalirin-7 might act as a scaffold to maintain normal level of NLGN3 surface expression. Disrupted S725 phosphorylation therefore could retain NLGN3 surface expression. Subsequent molecular studies are needed to identify the neuromodulatory signaling pathways that are affected by the NLGN3 and Kalirin-7 interaction.

We showed that both NLGN3 S725A and S725D mutations increase NLGN3 surface expression in cultured hippocampal neurons (Fig. 4), indicating the requirement of the serine residue for the regulation of NLGN3 trafficking. This is consistent with dynamic phosphorylation and dephosphorylation being essential for efficient surface expression. Since Cdk5-mediated phosphorylation has been known to regulate the surface expression of several membrane proteins (Dhavan and Tsai, 2001; Wang et al., 2003; Zhang et al., 2008; Jeong et al., 2013), our data indicate that NLGN3 is also regulated by the Cdk5-mediated membrane protein trafficking pathway. A study showed that NLGN2 S714A and S714D, NLGN2 PKA phospho-null and phospho-mimic mutants, both also displayed increased surface expression (Halff et al., 2022). Although the detailed molecular mechanism underlying the trafficking of NLGNs has not been fully identified, all these results indicate that the intact phosphorylation on the conserved serine residue in NLGNs is important for the regulation of NLGN trafficking.

To explore the functional relevance of the NLGN3 S725 phosphorylation, excitatory and inhibitory synaptic transmission was examined. We observed that both NLGN3 S725A and NLGN3 S725D significantly increase AMPAR-mediated mEPSC frequency compared with NLGN3 WT, which was not the case for AMPAR-mediated mEPSC amplitude (Fig. 6*C*). Several previous studies showed the positive correlation between NLGN surface expression levels and excitatory synaptic currents (Bemben et al., 2014; Jeong et al., 2019). Since we showed NLGN3 S725 mutants display increased surface expression levels (Fig. 4), it is possible that increased NLGN3 S725A and S725D surface expression enhances AMPAR-mediated mEPSC frequency in cultured neurons (Fig. 6). In contrast to the excitatory synaptic transmission, NLGN3 S725A and S725D both fail to rescue the GABAR-mediated mIPSC frequency (Fig. 7), which is quite interesting because that may reflect excitatory and inhibitory imbalance resulting from the disrupted S725 phosphorylation. As we found NLGN3

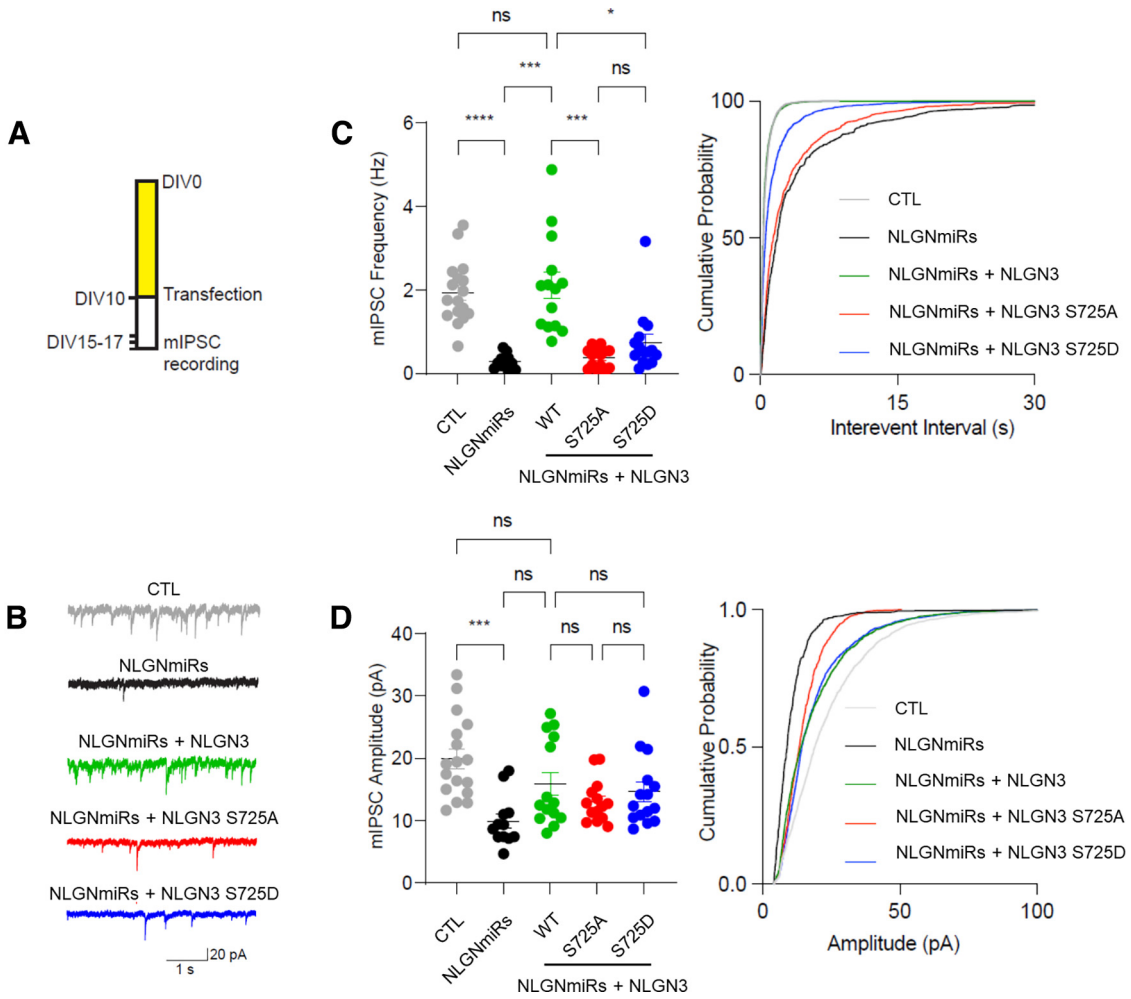

Figure 7. NLGN3 S725 is involved in inhibitory synaptic transmission. ***A***, Cultured hippocampal neurons were transfected at DIV 10, and mIPSC recording was performed at DIV 15-17. ***B***, Representative $GABA_AR$ mIPSC sample traces were recorded in cultured rat hippocampal neurons expressing either control neurons or transfected with NLGN miRs or NLGN miRs and HA-NLGN3 (WT, S725A, or S725D). ***C***, The mIPSC mean frequency and cumulative probability. ***D***, The mIPSC mean amplitude and cumulative probability. Error bar indicates SEM. $*p < 0.05$. $**p < 0.01$. $***p < 0.001$. $****p < 0.0001$. Data are representative of five independent experiments. The statistical significance between every condition was calculated using one-way ANOVA with Brown-Forsythe and Welch test for multiple comparisons.

S725A and S725D mutations do not disrupt the NLGN3 interaction with the postsynaptic scaffolding proteins (Fig. 3), these may not be because of the remodeling of postsynaptic protein complex. Instead, increased surface NLGN3 expression and reduced Kalirin-7 binding could abolish the fine regulation on synaptic transmission by a yet unidentified downstream mechanism, which leads to the disrupted synaptic transmission. In a previous study, Tabuchi et al. (2007) showed that, when an autism-associated NLGN3 R451C mutation is introduced into mice, the mutation impaired NLGN3 expression but increased inhibitory synaptic transmission without apparent change in excitatory synapses. All these implicate the intimate and complex regulatory mechanisms underlying the NLGN3 surface expression and synaptic function.

In this study, phospho-null (S725A) and phosphomimetic (S725D) mutations exert identical effects on NLGN3 binding with the PSD-95, Gephyrin, and Kalirin-7 (Fig. 3), NLGN3 surface expression (Fig. 4), and NLGN3-mediated synaptic transmission (Figs. 6, 7). These might be similar phenotypes caused by distinct disruptions of the phospho-site or molecular mechanisms that are not fully revealed. Detailed biochemical and molecular experiments would be required to characterize precise differences in the physiological function of NLGN3 S725A and S725D, although we believe our results reflect the importance of the intact phosphorylation site S725 allowing for dynamic phosphorylation and dephosphorylation for the physiological function of NLGN3.

Multiple studies report the identification of phosphorylation sites in the intracellular tail of NLGN isoforms and reveal that differential phosphorylation within the conserved region regulates NLGN isoform-specific functions (Bemben et al., 2014, 2015a,b; Jeong et al., 2017, 2019; Halff et al., 2022). However, any possible crosstalk between these phosphorylations has not been clearly identified. We do not exclude any possible crosstalk between S725 phosphorylation and other phosphorylation or modification sites on NLGN3, but extensive molecular studies should be undertaken to answer the question. Furthermore, since the PSD consists of a large complex of synaptic proteins, the effect of phosphorylation on the different NLGN-isoforms can be complicated to delineate *in vivo*. Nevertheless, our study identifies NLGNs as a novel Cdk5 substrate, shows binding throughout development, and reveals the functional consequences of the Cdk5-mediated NLGN3 phosphorylation. As the important roles of NLGN3 and Cdk5 in neurodevelopmental signaling and the pathophysiology of neurologic disorders have been reported independently, our current findings provide a converging

neuromodulatory signaling pathway to expand our understanding of the mechanisms underlying NLGN-mediated synapse regulation.

References

Antonelli R, Pizzarelli R, Pedroni A, Fritschy JM, Del Sal G, Cherubini E, Zacchi P (2014) Pin1-dependent signalling negatively affects GABAergic transmission by modulating neuroligin2/gephyrin interaction. Nat Commun 5:5066.

Baumann K, Mandelkow EM, Biernat J, Piwnica-Worms H, Mandelkow E (1993) Abnormal Alzheimer-like phosphorylation of tau-protein by cyclin-dependent kinases cdk2 and cdk5. FEBS Lett 336:417–424.

Bemben MA, Shipman SL, Hirai T, Herring BE, Li Y, Badger JD 2nd, Nicoll RA, Diamond JS, Roche KW (2014) CaMKII phosphorylation of neuroligin-1 regulates excitatory synapses. Nat Neurosci 17:56–64.

Bemben MA, Shipman SL, Nicoll RA, Roche KW (2015a) The cellular and molecular landscape of neuroligins. Trends Neurosci 38:496–505.

Bemben MA, Nguyen QA, Wang T, Li Y, Nicoll RA, Roche KW (2015b) Autism-associated mutation inhibits protein kinase C-mediated neuroligin-4X enhancement of excitatory synapses. Proc Natl Acad Sci USA 112:2551–2556.

Bibb JA, Snyder GL, Nishi A, Yan Z, Meijer L, Fienberg AA, Tsai LH, Kwon YT, Girault JA, Czernik AJ, Huganir RL, Hemmings HC Jr, Nairn AC, Greengard P (1999) Phosphorylation of DARPP-32 by Cdk5 modulates dopamine signalling in neurons. Nature 402:669–671.

Biederer T, Sara Y, Mozhayeva M, Atasoy D, Liu X, Kavalali ET, Sudhof TC (2002) SynCAM, a synaptic adhesion molecule that drives synapse assembly. Science 297:1525–1531.

Budreck EC, Scheiffele P (2007) Neuroligin-3 is a neuronal adhesion protein at GABAergic and glutamatergic synapses. Eur J Neurosci 26:1738–1748.

Budreck EC, Kwon OB, Jung JH, Baudouin S, Thommen A, Kim HS, Fukazawa Y, Harada H, Tabuchi K, Shigemoto R, Scheiffele P, Kim JH (2013) Neuroligin-1 controls synaptic abundance of NMDA-type glutamate receptors through extracellular coupling. Proc Natl Acad Sci USA 110:725–730.

Cruz JC, Tsai LH (2004) Cdk5 deregulation in the pathogenesis of Alzheimer's disease. Trends Mol Med 10:452–458.

Dean C, Scholl FG, Choih J, DeMaria S, Berger J, Isacoff E, Scheiffele P (2003) Neurexin mediates the assembly of presynaptic terminals. Nat Neurosci 6:708–716.

Dhavan R, Tsai LH (2001) A decade of CDK5. Nat Rev Mol Cell Biol 2:749–759.

Giannone G, Mondin M, Grillo-Bosch D, Tessier B, Saint-Michel E, Czondor K, Sainlos M, Choquet D, Thoumine O (2013) Neurexin-1beta binding to neuroligin-1 triggers the preferential recruitment of PSD-95 versus gephyrin through tyrosine phosphorylation of neuroligin-1. Cell Rep 3:1996–2007.

Haas KT, Compans B, Letellier M, Bartol TM, Grillo-Bosch D, Sejnowski TJ, Sainlos M, Choquet D, Thoumine O, Hosy E (2018) Pre-post synaptic alignment through neuroligin-1 tunes synaptic transmission efficiency. Elife 7:e31755.

Halff EF, Hannan S, Kwanthongdee J, Lesept F, Smart TG, Kittler JT (2022) Phosphorylation of neuroligin-2 by PKA regulates its cell surface abundance and synaptic stabilization. Sci Signal 15:eabg2505.

Herring BE, Nicoll RA (2016) Kalirin and Trio proteins serve critical roles in excitatory synaptic transmission and LTP. Proc Natl Acad Sci USA 113:2264–2269.

Hur EM, Zhou FQ (2010) GSK3 signalling in neural development. Nat Rev Neurosci 11:539–551.

Ichtchenko K, Hata Y, Nguyen T, Ullrich B, Missler M, Moomaw C, Sudhof TC (1995) Neuroligin 1: a splice site-specific ligand for beta-neurexins. Cell 81:435–443.

Irie M, Hata Y, Takeuchi M, Ichtchenko K, Toyoda A, Hirao K, Takai Y, Rosahl TW, Sudhof TC (1997) Binding of neuroligins to PSD-95. Science 277:1511–1515.

Jeong J, Park YU, Kim DK, Lee S, Kwak Y, Lee SA, Lee H, Suh YH, Gho YS, Hwang D, Park SK (2013) Cdk5 phosphorylates dopamine D2 receptor and attenuates downstream signaling. PLoS One 8:e84482.

Jeong J, Paskus JD, Roche KW (2017) Posttranslational modifications of neuroligins regulate neuronal and glial signaling. Curr Opin Neurobiol 45:130–138.

Jeong J, Pandey S, Li Y, Badger JD 2nd, Lu W, Roche KW (2019) PSD-95 binding dynamically regulates NLGN1 trafficking and function. Proc Natl Acad Sci USA 116:12035–12044.

Kim Y, Sung JY, Ceglia I, Lee KW, Ahn JH, Halford JM, Kim AM, Kwak SP, Park JB, Ho Ryu S, Schenck A, Bardoni B, Scott JD, Nairn AC, Greengard P (2006) Phosphorylation of WAVE1 regulates actin polymerization and dendritic spine morphology. Nature 442:814–817.

Kwon YT, Gupta A, Zhou Y, Nikolic M, Tsai LH (2000) Regulation of N-cadherin-mediated adhesion by the p35-Cdk5 kinase. Curr Biol 10:363–372.

Li BS, Zhang L, Gu J, Amin ND, Pant HC (2000) Integrin alpha(1) beta(1)-mediated activation of cyclin-dependent kinase 5 activity is involved in neurite outgrowth and human neurofilament protein H Lys-Ser-Pro tail domain phosphorylation. J Neurosci 20:6055–6062.

Liang Z, Zhan Y, Shen Y, Wong CC, Yates JR 3rd, Plattner F, Lai KO, Ip NY (2016) The pseudokinase CaMKv is required for the activity-dependent maintenance of dendritic spines. Nat Commun 7:13282.

Morabito MA, Sheng M, Tsai LH (2004) Cyclin-dependent kinase 5 phosphorylates the N-terminal domain of the postsynaptic density protein PSD-95 in neurons. J Neurosci 24:865–876.

Moy LY, Tsai LH (2004) Cyclin-dependent kinase 5 phosphorylates serine 31 of tyrosine hydroxylase and regulates its stability. J Biol Chem 279:54487–54493.

Nguyen T, Sudhof TC (1997) Binding properties of neuroligin 1 and neurexin 1beta reveal function as heterophilic cell adhesion molecules. J Biol Chem 272:26032–26039.

Paskus JD, Tian C, Fingleton E, Shen C, Chen X, Li Y, Myers SA, Badger JD 2nd, Bemben MA, Herring BE, Roche KW (2019) Synaptic Kalirin-7 and Trio interactomes reveal a GEF protein-dependent neuroligin-1 mechanism of action. Cell Rep 29:2944–2952.e2945.

Patrick GN, Zukerberg L, Nikolic M, de la Monte S, Dikkes P, Tsai LH (1999) Conversion of p35 to p25 deregulates Cdk5 activity and promotes neurodegeneration. Nature 402:615–622.

Penzes P, Jones KA (2008) Dendritic spine dynamics: a key role for kalirin-7. Trends Neurosci 31:419–427.

Penzes P, Johnson RC, Alam MR, Kambampati V, Mains RE, Eipper BA (2000) An isoform of kalirin, a brain-specific GDP/GTP exchange factor, is enriched in the postsynaptic density fraction. J Biol Chem 275:6395–6403.

Samuels BA, Hsueh YP, Shu T, Liang H, Tseng HC, Hong CJ, Su SC, Volker J, Neve RL, Yue DT, Tsai LH (2007) Cdk5 promotes synaptogenesis by regulating the subcellular distribution of the MAGUK family member CASK. Neuron 56:823–837.

Sanz-Clemente A, Matta JA, Isaac JT, Roche KW (2010) Casein kinase 2 regulates the NR2 subunit composition of synaptic NMDA receptors. Neuron 67:984–996.

Sara Y, Biederer T, Atasoy D, Chubykin A, Mozhayeva MG, Sudhof TC, Kavalali ET (2005) Selective capability of SynCAM and neuroligin for functional synapse assembly. J Neurosci 25:260–270.

Scheiffele P, Fan J, Choih J, Fetter R, Serafini T (2000) Neuroligin expressed in nonneuronal cells triggers presynaptic development in contacting axons. Cell 101:657–669.

Shipman SL, Schnell E, Hirai T, Chen BS, Roche KW, Nicoll RA (2011) Functional dependence of neuroligin on a new non-PDZ intracellular domain. Nat Neurosci 14:718–726.

Song JY, Ichtchenko K, Sudhof TC, Brose N (1999) Neuroligin 1 is a postsynaptic cell-adhesion molecule of excitatory synapses. Proc Natl Acad Sci USA 96:1100–1105.

Spafford JD, Zamponi GW (2003) Functional interactions between presynaptic calcium channels and the neurotransmitter release machinery. Curr Opin Neurobiol 13:308–314.

Tabuchi K, Blundell J, Etherton MR, Hammer RE, Liu X, Powell CM, Sudhof TC (2007) A neuroligin-3 mutation implicated in autism increases inhibitory synaptic transmission in mice. Science 318:71–76.

Tashiro A, Minden A, Yuste R (2000) Regulation of dendritic spine morphology by the rho family of small GTPases: antagonistic roles of Rac and Rho. Cereb Cortex 10:927–938.

Tsai LH, Delalle I, Caviness VS Jr, Chae T, Harlow E (1994) p35 is a neural-specific regulatory subunit of cyclin-dependent kinase 5. Nature 371:419–423.

Varoqueaux F, Jamain S, Brose N (2004) Neuroligin 2 is exclusively localized to inhibitory synapses. Eur J Cell Biol 83:449–456.

Varoqueaux F, Aramuni G, Rawson RL, Mohrmann R, Missler M, Gottmann K, Zhang W, Sudhof TC, Brose N (2006) Neuroligins determine synapse maturation and function. Neuron 51:741–754.

Vieira MM, Jeong J, Roche KW (2021) The role of NMDA receptor and neuroligin rare variants in synaptic dysfunction underlying neurodevelopmental disorders. Curr Opin Neurobiol 69:93–104.

Wang J, Liu S, Fu Y, Wang JH, Lu Y (2003) Cdk5 activation induces hippocampal CA1 cell death by directly phosphorylating NMDA receptors. Nat Neurosci 6:1039–1047.

Won S, Incontro S, Nicoll RA, Roche KW (2016) PSD-95 stabilizes NMDA receptors by inducing the degradation of STEP61. Proc Natl Acad Sci USA 113:E4736–E4744.

Xie Z, Srivastava DP, Photowala H, Kai L, Cahill ME, Woolfrey KM, Shum CY, Surmeier DJ, Penzes P (2007) Kalirin-7 controls activity-dependent structural and functional plasticity of dendritic spines. Neuron 56:640–656.

Zhang S, Edelmann L, Liu J, Crandall JE, Morabito MA (2008) Cdk5 regulates the phosphorylation of tyrosine 1472 NR2B and the surface expression of NMDA receptors. J Neurosci 28:415–424.